Pharm Res (2017) 34:957–970
DOI 10.1007/s11095-016-2046-6

RESEARCH PAPER

Elucidation of Compression-Induced Surface Crystallization in Amorphous Tablets Using Sum Frequency Generation (SFG) Microscopy

Pei T. Mah[1,2] • Dunja Novakovic[2] • Jukka Saarinen[2] • Stijn Van Landeghem[2] • Leena Peltonen[2] • Timo Laaksonen[3,4] • Antti Isomäki[5] • Clare J. Strachan[2]

Received: 29 June 2016 / Accepted: 3 October 2016 / Published online: 13 October 2016

ABSTRACT

Purpose To investigate the effect of compression on the crystallization behavior in amorphous tablets using sum frequency generation (SFG) microscopy imaging and more established analytical methods.

Method Tablets containing neat amorphous griseofulvin with/without excipients (silica, hydroxypropyl methylcellulose acetate succinate (HPMCAS), microcrystalline cellulose (MCC) and polyethylene glycol (PEG)) were prepared. They were analyzed upon preparation and storage using attenuated total reflectance Fourier transform infrared (ATR-FTIR) spectroscopy, scanning electron microscopy (SEM) and SFG microscopy.

Results Compression-induced crystallization occurred predominantly on the surface of the neat amorphous griseofulvin tablets, with minimal crystallinity being detected in the core of the tablets. The presence of various types of excipients was not able to mitigate the compression-induced surface crystallization of the amorphous griseofulvin tablets. However, the excipients affected the crystallization rate of amorphous griseofulvin in the core of the tablet upon compression and storage.

Conclusions SFG microscopy can be used in combination with ATR-FTIR spectroscopy and SEM to understand the crystallization behaviour of amorphous tablets upon compression and storage. When selecting excipients for amorphous formulations, it is important to consider the effect of the excipients on the physical stability of the amorphous formulations.

KEY WORDS amorphous · attenuated total reflectance Fourier transform infrared (ATR-FTIR) spectroscopy · compression · crystallization · griseofulvin · scanning electron microscopy (SEM) · sum frequency generation (SFG) microscopy

Dunja Novakovic and Jukka Saarinen contributed equally to this work.

Electronic supplementary material The online version of this article (doi:10.1007/s11095-016-2046-6) contains supplementary material, which is available to authorized users.

✉ Antti Isomäki
antti.isomaki@helsinki.fi

1 School of Pharmacy, University of Otago, Dunedin, New Zealand

2 Division of Pharmaceutical Chemistry and Technology, Faculty of Pharmacy, University of Helsinki, Helsinki, Finland

3 Division of Pharmaceutical Biosciences, Faculty of Pharmacy, University of Helsinki, Helsinki, Finland

4 Department of Chemistry and Bioengineering, Faculty of Natural Sciences, Tampere University of Technology, Tampere, Finland

5 Biomedicum Imaging Unit, Department of Anatomy, Medicum, Faculty of Medicine, FIN-00014 University of Helsinki, Haartmaninkatu 8, P.O. Box 63, Helsinki, Finland

ABBREVIATIONS

ATR-FTIR	Attenuated total reflectance Fourier transform infrared
DSC	Differential scanning calorimetry
HPMCAS	Hydroxypropyl methylcellulose acetate succinate
HyD	Hybrid detector
IR	Infrared
MCC	Microcrystalline cellulose
NMR	Nuclear magnetic resonance
OPO	Optical parametric oscillator
PEG	Polyethylene glycol
PMT	Photomultiplier tube
SEM	Scanning electron microscopy
SFG	Sum frequency generation
SHG	Second harmonic generation
XRPD	X-ray powder diffractometry

INTRODUCTION

Oral dosage forms are popular among patients as they are convenient and easy to administer. It is challenging to formulate new chemical entities into oral dosage forms as the majority of them are poorly water soluble (1,2). This has led to the development of various strategies to overcome this issue (3–7) and one of the promising strategies is to formulate drugs into the amorphous form (8–10). The disordered amorphous form has a higher solubility than its ordered crystalline counterpart (11,12). One of the major shortcomings of amorphous form that hinders its development is the tendency of the amorphous form to recrystallize back to the crystalline form (11,12), thus negating the solubility advantage of the amorphous form.

Tablets constitute more than 80% of the medicine market (9). One of the major processing steps in producing tablets is the compression step. Compression has been previously shown to induce crystallization in amorphous systems (13,14). It is important to gain an understanding of the effect of the compression parameters on the physical stability of amorphous formulations in order to optimize the compression step and to develop process control strategies. The use of analytical tools to detect crystallinity is needed to achieve this understanding. There is a myriad of analytical tools that have been commonly used to detect crystallinity and they include X-ray powder diffractometry (XRPD), differential scanning calorimetry (DSC) and vibrational spectroscopies (i.e. infrared, Raman and nuclear magnetic resonance (NMR) spectroscopies) (15,16). However, these analytical tools do not generally provide information regarding the spatial distribution of the crystallization and this insight is crucial to elucidate process understanding. Raman microscopy has been previously used to map crystallinity distribution in pharmaceutical amorphous formulations (17,18). This imaging technique has its own set of drawbacks which include the requirement of leveled surfaces, long acquisition times (especially for Raman mapping which is much better suited than Raman global illumination imaging for resolving solid state forms) and the need for complicated data analysis.

Sum frequency generation (SFG) imaging is a potential analytical tool that can be applied to image crystallinity distribution in an amorphous matrix. SFG is a second order nonlinear optical process in which a single photon is generated with a frequency that is the sum of the two incident photons (19–21). A special case of SFG is second harmonic generation (SHG) which occurs when two photons of the same frequency sum together resulting in the generation of a photon with a frequency that is twice that of the incident photons (19–21). SFG can be used to probe both electronic and vibrational transitions in a medium. It is most commonly used in vibrational spectroscopy on surfaces where sum frequency of one visible beam and one mid-infrared (IR) beam is used to probe IR and Raman active vibrational transitions of molecules (22). In this study, however, we exploit the nonresonant SFG as an alternative to near-IR excited SHG. In terms of practical application, SHG is more commonly applied than SFG with two different input frequencies since the latter requires a setup with two temporally overlapped ultrashort pulse excitation lasers with different wavelengths which is more complicated than having one (21). On the other hand, the setup used here provides an option in future studies to concurrently perform coherent anti-Stokes Raman scattering (CARS) imaging which provides complementary information regarding the chemical composition of the sample (23). In such a multimodal setup SFG imaging offers several advantages when compared to SHG as discussed in detail in the "Materials and methods" section.

The possibility of using SHG in pharmaceutical settings to resolve amorphous from crystalline materials has been first demonstrated by Strachan *et al.* (24). In order to have SFG or SHG response, the sample should exhibit lack of phase inversion (i.e. its crystal structure is non-centrosymmetric) (19–21). Many pharmaceutically relevant crystalline materials do not have inversion symmetry and thus are expected to emit a second order nonlinear signal. Another condition that needs to be met is the phase-matching condition in which the pump signals need to combine in the right phase with the second order response in order to generate a detectable overall signal (19–21). Amorphous materials lack the long-range crystalline order needed for phase-matching and thus do not generate second order nonlinear signals.

The use of SHG has been combined with a microscope to image the distribution of crystallinity in amorphous materials (25–31). Wanapun *et al.* investigated the distribution and kinetics of crystallization of amorphous griseofulvin and chlorpromamide at temperatures above the drugs' respective glass transitions using SHG imaging and compared the onset of crystallizations with those obtained using polarized light microscope (PLM) (29). It was found that SHG imaging detected onset of crystallization earlier than PLM. In a later report, Wanapun *et al.* compared SHG imaging with XRPD in detecting trace crystallinity in milled amorphous griseofulvin system (30). SHG imaging was able to detect and quantify trace crystallinity in samples which were X-ray amorphous. Kestur *et al.* prepared naproxen-HPMCAS solid dispersion and found that SHG imaging detected crystallinity immediately after preparation which was not detected by XRPD and Raman spectroscopy, thus further demonstrating the superiority of SHG imaging in detecting trace crystallinity in comparison to other conventional non-spatially resolved techniques (31). They also stored the samples under accelerated conditions and compared the three techniques in quantifying crystallinity during the storage period. They found that the three techniques investigated predicted crystallinity values which generated similar kinetic profiles. SHG imaging has also been reported to be used to investigate other polymer based solid dispersion containing naproxen (28,32).

The main aim of this study was to use SFG imaging to evaluate crystallinity in amorphous tablets. Griseofulvin, which has antifungal properties (33), was used as the model drug of this study. There are three polymorphs (forms I, II, and III) that have been reported for griseofulvin (33). Amorphous griseofulvin prepared by quench cooling with a melting period less than 10 min has been consistently demonstrated to recrystallize to the crystalline form I, which consists of a tetragonal cell and a $P4_1$ space group that is non-centrosymmetric (29,30,34).

The first part of the study involved using SFG imaging to evaluate the distribution of crystallinity upon preparation and storage in neat amorphous griseofulvin tablets. The qualitative capability of SFG imaging in detecting low levels of crystallinity was also compared to attenuated total reflectance Fourier transform infrared (ATR-FTIR) spectroscopy and scanning electron microscopy (SEM). The second part of the study involved evaluating crystallinity distribution in amorphous griseofulvin tablets containing different pharmaceutical excipients. This part of the study is of high relevance in the area of pharmaceutical solid state research as pharmaceutical excipients are commonly incorporated into pharmaceutical products for a multitude of purposes which include to aid processing and to enhance the physical stability and dissolution performance of the product.

MATERIALS AND METHODS

Materials

Griseofulvin form I (Sigma-Aldrich, St. Louis, USA) was used as the model drug. The excipients used in this study were silica with particle size of 12 nm (Aerosil 200, Evonik Industries AG, Hanau-Wolfgang, Germany), hydroxypropyl methylcellulose acetate succinate MF (HPMCAS, Shin-Etsu Chemical Co., Tokyo, Japan), microcrystalline cellulose NF PH105 (MCC, FMC BioPolymer, Brussels, Belgium) and polyethylene glycol 6000 (PEG, Sigma-Aldrich, St. Louis, USA) and were used as received. Phosphorus pentoxide (Sigma-Aldrich, Steinheim, Germany) was used to create a storage condition of 0%RH.

Sample Preparation

Amorphous griseofulvin was prepared by quench cooling. This process involved heating a thin layer of crystalline griseofulvin to 10°C above its melting point and holding it at that temperature for 3 min. Liquid nitrogen was then rapidly poured onto the melt to kinetically trap the molecules in the disordered state. A previous report has shown that heating griseofulvin at 10°C above its melting point for 10 min did not result in any detectable chemical degradation as measured with ^{1}H NMR spectroscopy (33). Without any further processing, the amorphous griseofulvin layer was stored over phosphorous pentoxide for 1 h to remove any condensed water that developed during the rapid cooling stage. The amorphous griseofulvin layer was then gently pulverized to form a fine powder using the mortar and pestle. The neat amorphous griseofulvin powder was then compacted into tablet compacts using the Specac Hydraulic Press Model 15.011 (Specac, Kent, UK) equipped with a 13 mm diameter flat faced punch. The compacts were then formed with a compaction pressure of 58 MPa and a dwell time of 30 s.

A quench cooled mixture of griseofulvin and the amorphous silica was prepared using the following steps. Initially, crystalline griseofulvin and silica were mixed using the planetary ball mill Pulverisette 6 (Fritsch GmbH, Idar-Oberstein, Germany) to maximize homogenous mixing. Crystalline griseofulvin and silica were individually weighed (i.e. 1.5 g each) and placed in an 80 ml volume stainless steel bowl, containing 15 stainless steel balls (10 mm in diameter). The milling was carried out at 400 rpm for 3 min. Then, the powder mixture was thinly spread onto aluminium pans and quench cooled. The quench cooling procedure used for these samples was similar to the procedure used for the preparation of neat amorphous griseofulvin. However, liquid nitrogen was not used for the rapid cooling. Instead, the heated mixture was rapidly cooled at room temperature. The reason for the change in the rapid cooling method was because the heated mixture remained as powder and pouring liquid nitrogen over it resulted in displacement of the powder from the aluminium pan. The cooled mixture was then stored over phosphorus pentoxide until further processing. Tablet compacts of the cooled mixture were prepared using the same procedure described for neat amorphous griseofulvin tablets.

Binary mixtures of amorphous griseofulvin and various polymers were prepared by gently mixing neat amorphous griseofulvin powder (prepared using the procedures described above) and the polymer of interest in a 1:1 w/w ratio using the mortar and pestle. The excipients used in this part of the study were HPMCAS, MCC, and PEG. Tablets of the binary mixtures were prepared using the same tabletting procedure described for neat amorphous griseofulvin tablets.

ATR-FTIR Spectroscopy

Infrared spectroscopy measurements were conducted using a Bruker Vertex 70 spectrometer (Bruker Optik, Ettlingen, Germany) coupled with an ATR accessory, which consisted of a single reflection diamond crystal (MIRacle, Pike Technologies, Madison, WI, USA). The spectrometer consisted of a KBr beam splitter, a MIR source and a RT-DLaTGS detector. The final spectra were the mean of 64 scans with a spectral range from 650 to 4000 cm^{-1}. Interferograms were apodized with the Blackman-Harris 3-term function and subjected to Fourier transformation

generating spectra with a resolution of 4 cm^{-1}. The ATR spectra were converted to absorbance spectra using OPUS software (v. 5.0, Bruker Optik, Ettlingen, Germany).

ATR-FTIR spectroscopy was used to detect crystallinity in the neat amorphous griseofulvin tablets immediately after compression. Three different regions of each tablet were probed and the recorded spectra were visually examined for crystalline spectral features. A tablet is deemed to contain crystallinity upon the observation of any crystalline spectral features.

SFG Imaging

A Leica TCS SP8 CARS microscope (Leica Microsystems GmbH, Wetzlar, Germany) was used for SFG imaging and linear reflected light imaging. The instrument consists of an inverted microscope equipped with a laser-scanning confocal scan-head, two descanned high sensitivity hybrid GaAsP detectors (HyD) and one conventional photomultiplier tube (PMT). A single-photon HeNe 633 nm laser and the PMT detector were used for reflected light imaging. For the SFG imaging, a picoEmerald (A.P.E. GmbH, Berlin, Germany) light source was used. The integrated source combines a solid-state Nd:YVO_4 laser and a tunable picosecond optical parametric oscillator (OPO) having the pulse widths of 7 ps and 5–6 ps, respectively. The temporally overlapped pulses from the two sources have the repetition rate of 80 MHz. The fundamental wavelength of the laser at 1064.5 nm (λ_1) was used in combination with the 817 nm (λ_2) OPO output to generate a sum-frequency signal at 462 nm (λ_{SFG}) according to the following equation:

$$\lambda_{SFG} = \frac{1}{\frac{1}{\lambda_1} + \frac{1}{\lambda_2}} \quad (1)$$

The optimal excitation wavelengths for SHG and SFG depend on the sample properties and the detection sensitivity for the emitted signal wavelength. The material scattering length, dispersion, and the possible presence of electronic excited states close to the SHG or SFG frequencies affect the generated signal intensity in particular in reflected light detection geometry (35). Full characterization of these material properties was out of the scope of the present study. In the microscope setup used here the SFG emission peak at 462 nm allowed for taking advantage of the high quantum efficiency range of the HyD detectors. A strong SFG signal was detected from crystalline griseofulvin form I (Figure S1, supporting information). We also observed significantly lower autofluorescence background arising from the 1064.5 nm excitation when compared to the same signal level from the 817 nm excitation alone. Moreover, the 817-nm-excited autofluorescence background at the SFG signal wavelength can be conveniently measured by switching off the 1064.5 nm beam. This makes the background subtraction much more straightforward than in case of the SHG. It is also worth noting that the threshold for laser-induced damage is typically higher when longer wavelengths are applied (36). These damage mechanisms were not critical in the current study but they may become prominent in case of other types of samples such as biologics, tissue or living cells. Finally, the proper selection of the two excitation wavelengths offers a direct path to gain complementary information about the chemical composition using CARS imaging. For example, the difference frequency arising from the simultaneous excitation at 817 nm and 1064.5 nm corresponds to a molecular vibrational frequency of CH-bonds at 2845 cm^{-1}.

In all imaging modes, the laser light was focused on the sample for scanning using a 25X 0.95 N.A. water immersion HCX IRAPO L objective (Leica). The SFG signal was spectrally filtered using a tunable spectrophotometer at 450–470 nm and detected using a HyD detector.

A high precision galvanometric Z-stage was used for acquiring volumetric data and for scanning the samples with rough surface profiles. Maximum intensity projections of the Z-stacks were used for analysis. For acquiring images of large sample areas, a motorized XY-stage and a tile scan function were used. Tile scanning involved systematically moving the sample using a motorized stage and capturing an image at each position until the whole predefined area had been imaged. Then, a mosaic image was assembled by stitching the recorded images. The microscope was operated and all images were captured and analyzed using the Leica Application Suite Advanced Fluorescence (LAS AF) v.3.3 software (Leica Microsystems GmbH, Wetzlar, Germany). ImageJ was used for SFG area quantification. Images were thresholded (7–255) to exclude the detector noise and the remaining signal area was compared with the area of the surface reflection image using "Area fraction" measurement tool.

The flat surfaces of the tablets were imaged as such. As for the imaging of the cross-sections of the core of the tablets, the tablets were broken and mounted on the glass slides with the assistance of Blu-Tack. New freshly-broken cross-sections of the core of the tablets were imaged after the tablets had been stored.

SEM

The surfaces and the cross-sections of freshly prepared and stored amorphous griseofulvin tablets were imaged using SEM. The cross-sections of the tablets were obtained by cutting the tablets using a razor blade. The SEM images were recorded using the FEI Quanta 250 FEG (FEI Inc., Eindhoven, Netherlands) scanning electron microscope equipped with the Everhart-Thornley detector. A working voltage of 10 kV was used. The samples were mounted on aluminium stubs with double-sided carbon tape and were then coated with platinum before imaging.

Storage

Samples were stored in open vials at 30°C over phosphorus pentoxide (0%RH) and monitored using ATR-FTIR spectroscopy, SFG imaging and SEM.

RESULTS AND DISCUSSION

Tablets Containing Neat Amorphous Griseofulvin

Infrared spectra of the neat amorphous griseofulvin tablets were recorded upon compression of the tablets and visually compared to the spectra of amorphous and crystalline griseofulvin form I powder in order to determine whether compression had resulted in detectable crystallization of the tablet. Figure 1 shows the infrared spectra of crystalline and amorphous griseofulvin, as well as an example of the infrared spectra of a partially crystallized griseofulvin tablet. Whilst ATR-FTIR spectroscopy detected crystallinity in a portion of the freshly prepared tablets, some of the tablets did not exhibit crystallinity that could be detected by ATR-FTIR spectroscopy. A possible reason for the observations could be subsampling of the samples as the ATR-FTIR spectroscopy setup probes a small region of the surface (less than 8% of the surface of the tablet) during each measurement and crystallization was not homogenous across the surface of the tablet. It was also not possible to conclude from the ATR-FTIR spectroscopy results whether the crystallization upon compression was widespread throughout the tablet or did it only affect the surface of the tablet.

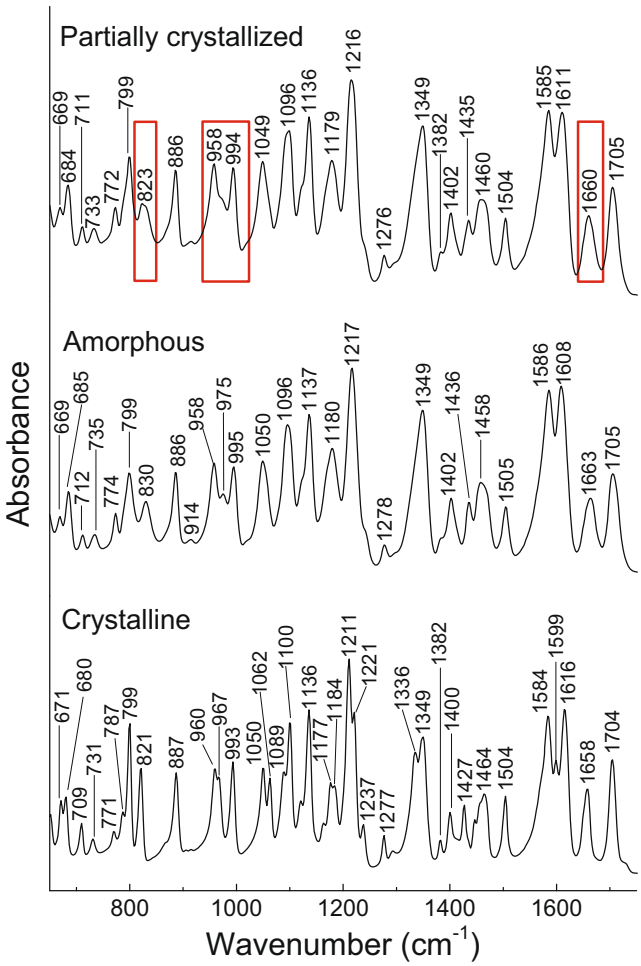

Figure 1 Infrared spectra of crystalline and amorphous form of griseofulvin and partially crystallized tablet. Spectral shifts and broadening of peaks were observed upon amorphization of griseofulvin. The highlighted regions of the spectrum of partially crystallized tablet indicate the spectral differences (i.e. crystallization) when compared to the amorphous griseofulvin spectrum.

SFG microscopy was utilized to provide insight into the crystallinity distribution of the griseofulvin tablets. The freshly prepared neat amorphous griseofulvin tablets that had been probed with ATR-FTIR spectroscopy were then divided into two groups as to whether crystallinity was absent (known as 'ND-FTIR') or present (known as 'D-FTIR') according to ATR-FTIR spectroscopy and studied using SFG microscopy. The SFG images of the surfaces and the cross-sections of the core of sample tablets 'ND-FTIR' and 'D-FTIR' on Day 0 (upon compression) and their corresponding reflection images are shown in Figs. 2 and S2 (supporting information). The SFG images demonstrate that crystallinity was present on the surfaces of both groups of tablets, even in tablets which were suggested to be crystal-free according to ATR-FTIR spectroscopy. Examination of the other areas on the tablets' surfaces using SFG microscopy suggested that the crystallinity on the surfaces was not evenly distributed with some regions having little crystallinity and some regions having widespread crystallinity. The tablets' cross-section images on day 0 show that there was minimal crystallinity in the core of the tablet suggesting that crystallization induced by the compression process used in this study predominantly occurred on the surface of the tablets.

The 'ND-FTIR' tablets were stored at 30°C/ 0%RH and the crystallization progression was monitored using SFG microscopy (Fig. 2) and SEM (Fig. 3). Crystalline-like features were not seen with SEM on the surfaces of the tablets upon compression. Signs of crystallinity (branch-like features) on the surfaces of the tablet which were apparent from the SEM images were observed on Day 2 and Day 5 of storage. The progression in crystallization in the core of the 'ND-FTIR' tablets was apparent from the SFG measurements that indicated about ten-fold increase in the crystalline area after five days of storage (from $0.6 \pm 0.4\%$ to $10.2 \pm 2.6\%$, $n = 3$ tablets). Sparsely distributed crystalline domains were observed in the core of the tablet on Day 0 and Day 2 of storage. The crystalline domains in the core of the tablet were more extensive

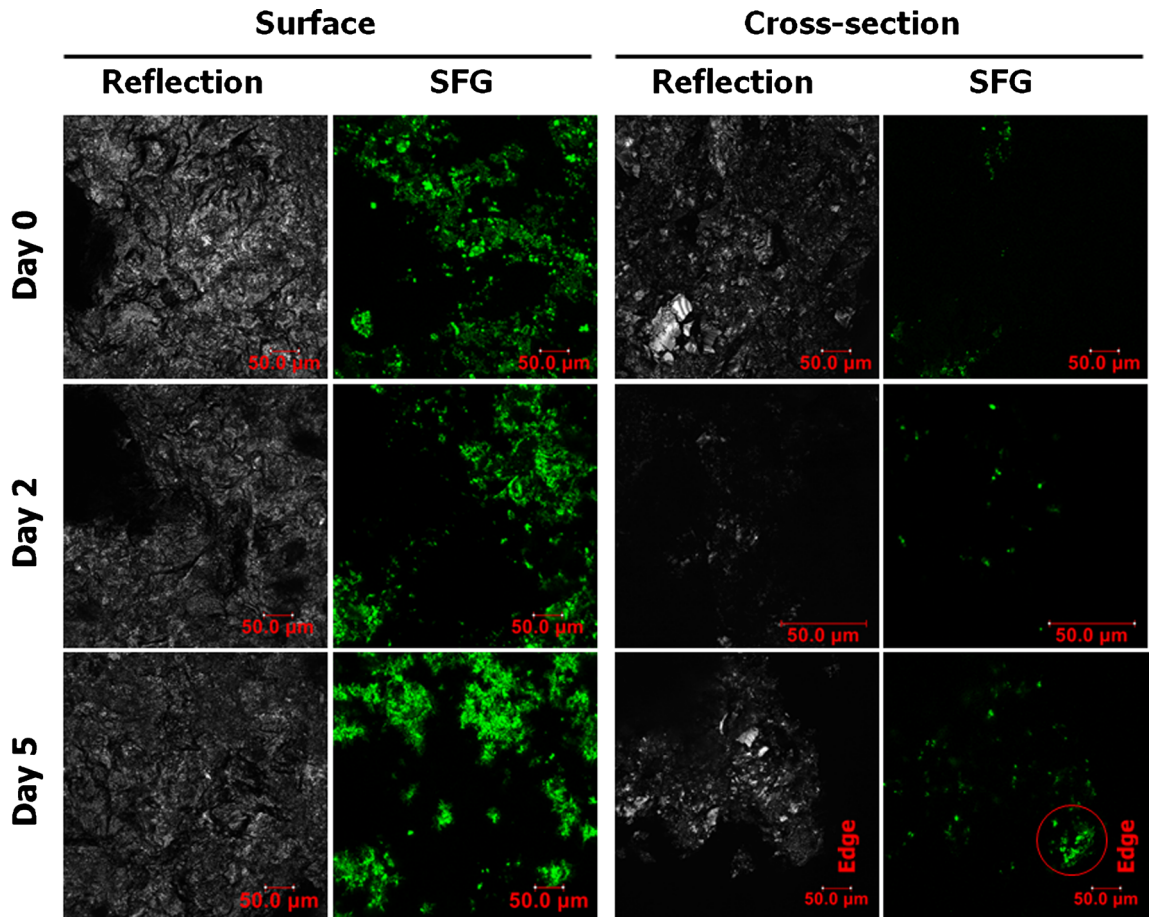

Figure 2 Reflection and SFG images of the surfaces and the cross-sections of a sample tablet of 'ND-FTIR' upon storage at 30°C/ 0%RH. SFG active crystalline regions (green) were observed already on day 0. The red outline highlights the crystalline regions near the surface edge of the tablet cross-section. The scale bars indicate 50 μm.

on Day 5 with large crystalline regions being observed near the surface edge of the tablet (highlighted in Fig. 2). Crystallinity was not detected by SEM in the core region of the tablet throughout the 5 days of storage as indicated by the smooth surfaces of the cross-sections of the tablet.

The results above demonstrate the use of a set techniques that provided complementary information to elucidate the crystallization behavior of amorphous griseofulvin tablets upon compression and storage. The ATR-FTIR spectroscopy setup had a spectral acquisition time of about a minute per spectrum. The technique is able to provide chemical as well as solid-state information within a sampling volume of approximately 1–2 µm into the sample and is commonly used to distinguish crystalline from amorphous materials. In this study, compression induced crystallization on the surfaces of a portion of freshly prepared amorphous tablets was detectable using ATR-FTIR spectroscopy. SFG microscopy was used to investigate the crystallinity distribution in the tablets and also to further provide an understanding as to why ATR-FTIR spectroscopy only detected crystallization upon compression in certain tablets. The data acquisition time of SFG microscopy was short (i.e. a few minutes for an image) and no complicated data analysis was required to process the images. It was found with SFG microscopy that crystallization was not uniform on the surface of the tablets and this explains the variable results obtained using ATR-FTIR spectroscopy. The SFG images demonstrate that crystallization on the surface of the tablets progressed faster than that in the core of the tablets. SEM was used to provide information regarding the morphology of the crystals.

It can be concluded from the above results that compression caused nucleation on the surface of the amorphous griseofulvin tablets. The nuclei induced by compression did not have a distinct shape. However, compression did not induce crystallization in the core of the tablets. The presence of widespread nuclei on the surfaces of the tablets triggered rapid surface crystal growth and this explains the differences in crystallization rates observed between the surfaces and the core of the tablets. This is further supported by the crystal features observed using SEM, where branch like features suggest crystal growth from a limited number of nuclei.

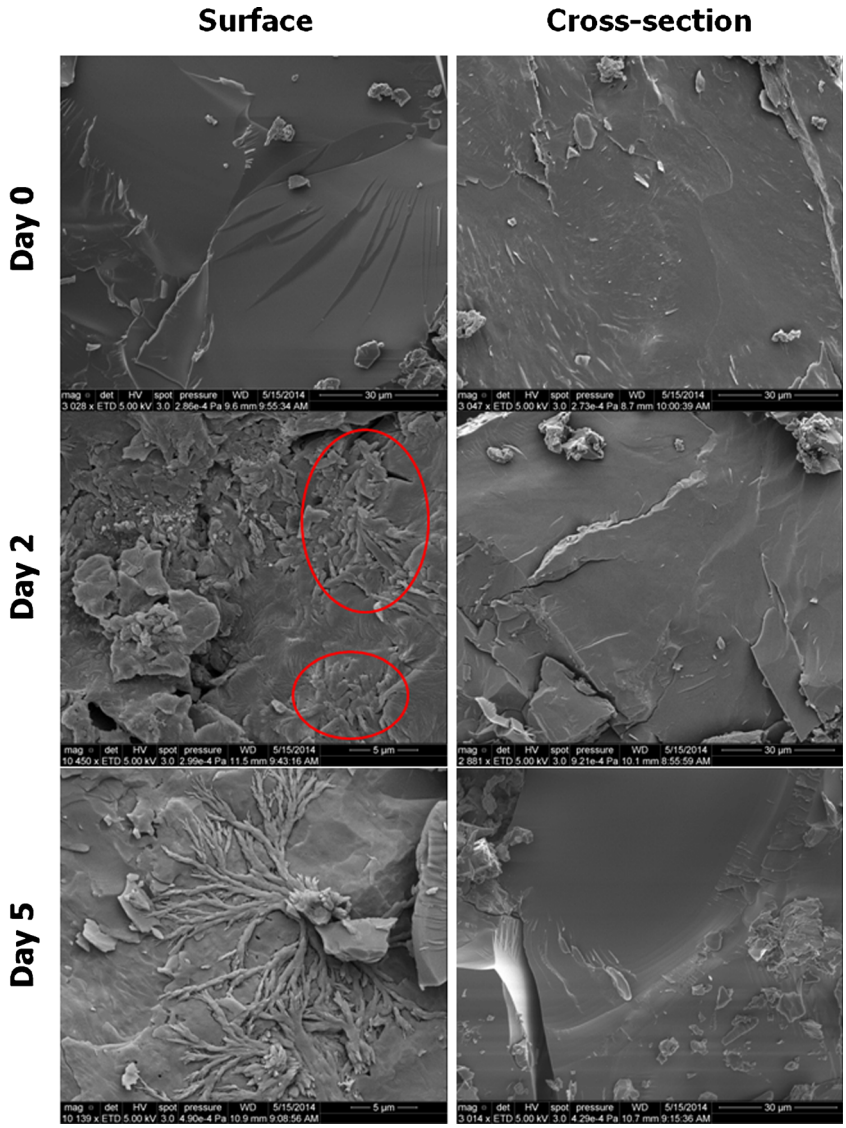

Figure 3 SEM images of the surfaces and the cross-sections of a sample tablet 'ND-FTIR' upon storage at 30°C/ 0%RH. The regions outlined in red indicate crystalline regions.

Tablets Containing Amorphous Griseofulvin and Polymer Excipients

Excipients are added into pharmaceutical formulations to aid processing and to enhance physical stability and dissolution performance. The aim of the next part of the study was to utilize SFG microscopy to detect crystallization of griseofulvin in binary component tablets containing griseofulvin and an excipient. The excipients used in this study were silica and various polymers, which included HPMCAS, MCC and PEG. Amorphous griseofulvin tablets containing silica were prepared using a quench cooled mixture of silica and crystalline griseofulvin in 1:1 w/w ratio. Amorphous griseofulvin tablets containing the various polymers were prepared using physical mixtures of neat amorphous griseofulvin and the polymer of interest (1:1 w/w ratio). The reason the polymers were physically mixed with amorphous griseofulvin, rather than being quench cooled together with crystalline griseofulvin was because these excipients chemically degraded upon being heated to a temperature slightly above the melting point of crystalline griseofulvin.

Quench Cooled Mixture of Non-porous Nanoparticulate Silica and Griseofulvin

This part of the study involves utilizing SFG microscopy to detect early signs of crystallization in tablets containing a quench cooled mixture of silica and griseofulvin in a 1:1 w/w ratio. The silica used in this study is non-porous in nature and has a particle size of 12 nm. Silica, which is amorphous in nature, is centrosymmetric and thus is not SFG active. This was confirmed by the SFG measurements of silica in the powder and tablet forms. Studies have shown that quench cooling silica with a drug was able to slow down the crystallization rate of amorphous formulations upon storage (37,38). The infrared spectrum of the quench cooled mixture of griseofulvin and silica was recorded

and compared to the spectra of crystalline and neat amorphous griseofulvin (Figure S3 (supporting information)) in order to determine the solid state of the quench cooled mixture. The spectrum of the quench cooled mixture had close resemblance to the spectrum of amorphous griseofulvin. However, close examination revealed that there were slight shifts in the peaks, and the ratio of the peak intensities at 1589 cm^{-1} and 1613 cm^{-1} of the quench cooled mixture was different from the corresponding peak intensities ratio of neat amorphous griseofulvin. These differences were not attributed to silica as silica did not exhibit any spectral features in the examined spectral region. The differences could be due to the presence of molecular interactions between griseofulvin and silica. Silica has been previously shown to form molecular interactions with other drugs upon fusion, ball milling and spray drying (37–39). The quench cooled mixture also did not emit any SFG signal, further confirming the amorphous nature of the sample.

The SFG images of the surfaces and cross-sections of the tablet of quench cooled mixture and their corresponding reflection images upon preparation and storage at 30°C/ 0%RH are shown in Fig. 4. In order to provide a better representation of the crystallinity distribution in the tablet, SFG images of two different sites of the tablet's surface and cross-section are shown. Upon compression (i.e. Day 0), crystallinity was detected on the surface of the tablet with some sites having minimal crystallinity (illustrated by Site 1) and some sites having large crystalline domains (illustrated by Site 2). The SFG images of the cross-section of the tablet show that crystalline domains were only found on the surface edge of the tablet and not in the core of the tablet. These results are similar to those of neat amorphous griseofulvin tablets, suggesting that quench cooling griseofulvin and silica was not able to prevent compression-induced crystallization on the surface of the tablet. Storing the tablet at 30°C/ 0%RH for 6 days resulted in the progression of crystallization with the observation of larger and more extensive crystalline domains on the surface of the tablet. Sparsely distributed crystalline spots were observed in the core of the tablet on Day 6 of storage. Comparison of these results with those of neat amorphous griseofulvin tablets revealed that quench cooling griseofulvin with silica resulted in a decrease in the core crystallization rate. No crystalline-like features were found in the SEM images

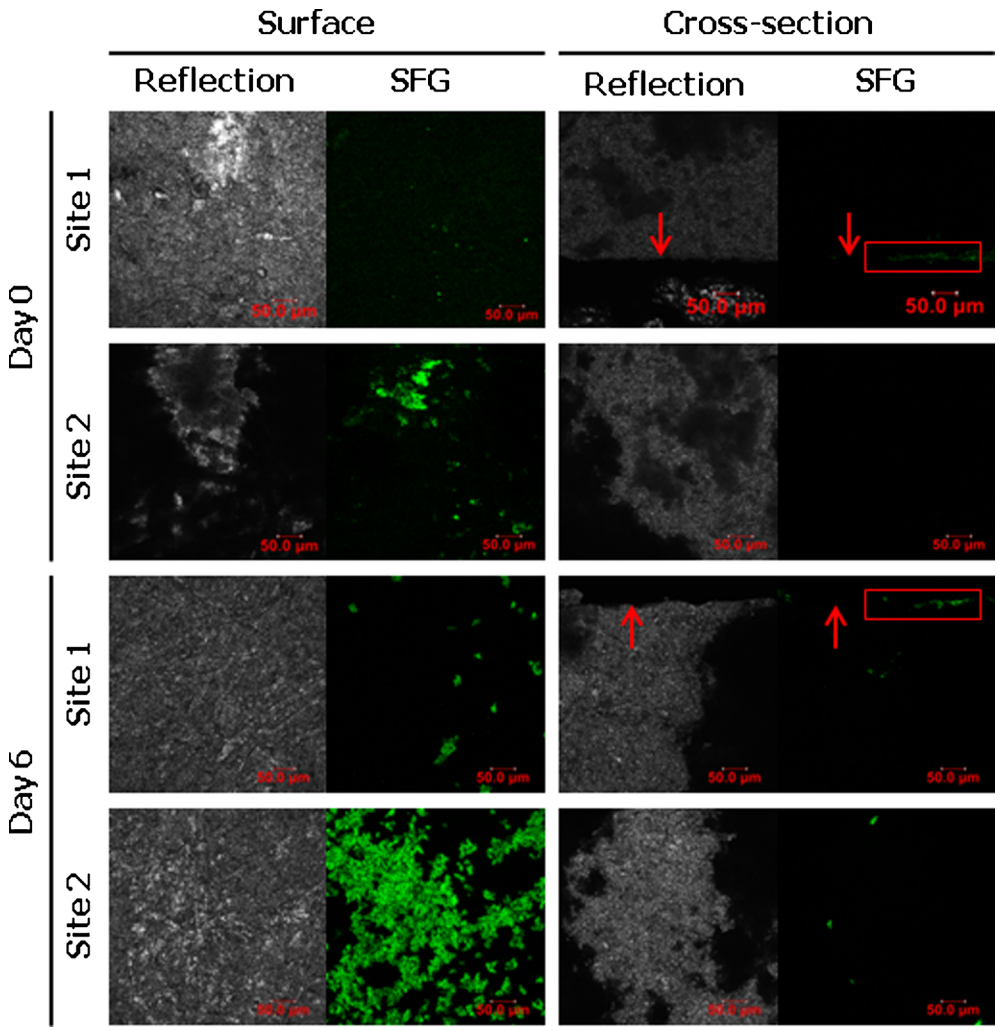

Figure 4 Reflection and SFG images of the surfaces and the cross-sections of a tablet containing quench cooled mixture of silica and griseofulvin (1:1 w/w ratio) upon storage at 30°C/ 0%RH. The SFG signals (green) indicate crystalline regions. The *red arrows* indicate the surface edge of the tablets. The red rectangles highlight the regions with low levels of crystallinity as indicated by the faint green colour. The scale bars indicate 50 μm.

(Figure S4 (supporting information)) of the stored tablet of the quench cooled mixture. ATR-FTIR spectroscopy was not utilized to evaluate crystallinity in the tablet of the quench cooled mixture as ATR-FTIR spectroscopy does not provide spatial information and has been demonstrated above to be less capable than SFG in detecting low levels of crystallinity.

In order to further investigate the effect of mechanical compression on the distribution of the crystallization, tablets of quench cooled mixture of griseofulvin and silica were prepared using the configuration shown in Fig. 5a. The purpose of this configuration was to prepare tablets with two types of surfaces (i.e. one surface that was adjacent to the tablet punch and another surface that can be termed the 'core' surface). As the material adhered to the punch, pieces of weighing paper were placed in between the punches and the sample before compression. Another piece of paper was sandwiched in between two layers of the powder sample before compression in order to create 'core' surfaces that were flat, which facilitated SFG imaging of large regions. Even though technically there was a piece of paper between the punch and the sample, the tablet surface that was close to the punch was called the surface impinging the punch and the other surface of the same tablet was known as 'core' surface.

Tile scanning was performed on the surfaces of the tablet in order to image larger areas of the tablet to provide a better representation of the crystallinity distribution on the surfaces. The SFG mosaic images and their corresponding reflection images are shown in Fig. 6. The region on the surface impinging the punch that was imaged was close to the round edge of the tablet and it demonstrated widespread crystallinity. Examination of other regions on the same surface also revealed the presence of crystallinity. In contrast, the 'core' surface exhibited minimal crystallinity. As the resultant 'core' surface was not adequately levelled for the imaging of a large region close to the round edge of the tablet, separate tile scannings of different regions of the surface (as shown in Fig. 5b) were performed in order to obtain a representative crystallinity distribution. It can be seen that practically no crystallinity was present in the middle region of the 'core' surface of the tablet (i.e. Site 1 of Fig. 6). The SFG image of Site 2 of Fig. 6 also demonstrates that very minimal crystallinity was observed on the 'core' surface, except for a few crystalline domains. It can also be observed that the round edge of the 'core' surface of the tablet was lined with crystalline material. These results and those above (demonstrating compression-induced crystallization on the surface impinging the punch) could be due to the different compression force experienced by the material on different regions of the tablet compact. This phenomenon is confirmed by a report by Ellison *et al.* who demonstrated the uneven distribution of compression force in a tablet during the tablet making process (40). Nonuniform crystallization was also observed by Thakral *et al.* in amorphous indomethacin tablets upon 24 h of storage at 35°C (14). It was reported that greater amount of crystallinity was detected at the radial surface of the stored amorphous indomethacin tablets when compared to the core of the tablets. Thakral *et al.* attributed this observation to the occurrence of radial surface-die wall friction.

The above results demonstrate that large regions on the surfaces of tablets were successfully imaged in a relatively short period of time with each mosaic image taking approximately 45 min to acquire. This technique has a shorter acquisition time and requires very limited data analysis in order to obtain crystallinity distribution maps when compared to Raman microscopy.

Binary Mixtures of Neat Amorphous Griseofulvin and Various Polymers

The effect of different polymers on the crystallization behavior of neat amorphous griseofulvin upon compression and storage was investigated using SFG microscopy. SFG measurements of all the polymers in powder and tablet forms revealed that all the polymers did not emit SFG signal (Figure S5 (supporting information)). HPMCAS is amorphous in nature and thus is SFG inactive. It was not expected of MCC (semicrystalline in nature) to be SFG inactive as it has a monoclinic crystal system (space group $P2_1$) which is non-centrosymmetric (41). PEG, which is also semi-crystalline in nature, has a monoclinic crystal system with a space group of $P2_1/a$-$C_{2n}5$ which is centrosymmetric (42,43). These polymers were physically mixed with neat amorphous griseofulvin in a 1:1 w/w ratio before compression. Figure 7 shows the reflection and SFG images of the surfaces and the cross-sections of tablets containing binary mixtures of neat amorphous griseofulvin and various polymers upon storage at 30°C/ 0%RH. Crystallization of griseofulvin on the surface of the tablet upon compression (i.e. Day 0) was observed for all the tablets containing different polymers. The crystallization on the tablets containing PEG upon compression was observed on the whole surface of the tablet and was much more extensive than the crystallization on the surfaces of tablets containing HPMCAS and MCC. Examination of the

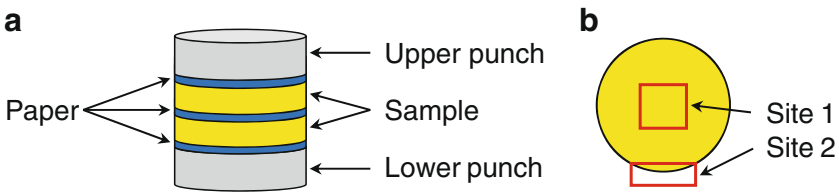

Figure 5 (**a**) The configuration of the preparation of tablets with a surface impinging the punch and a 'core' surface. (**b**) Locations of Sites 1 and 2 of the core surface imaged.

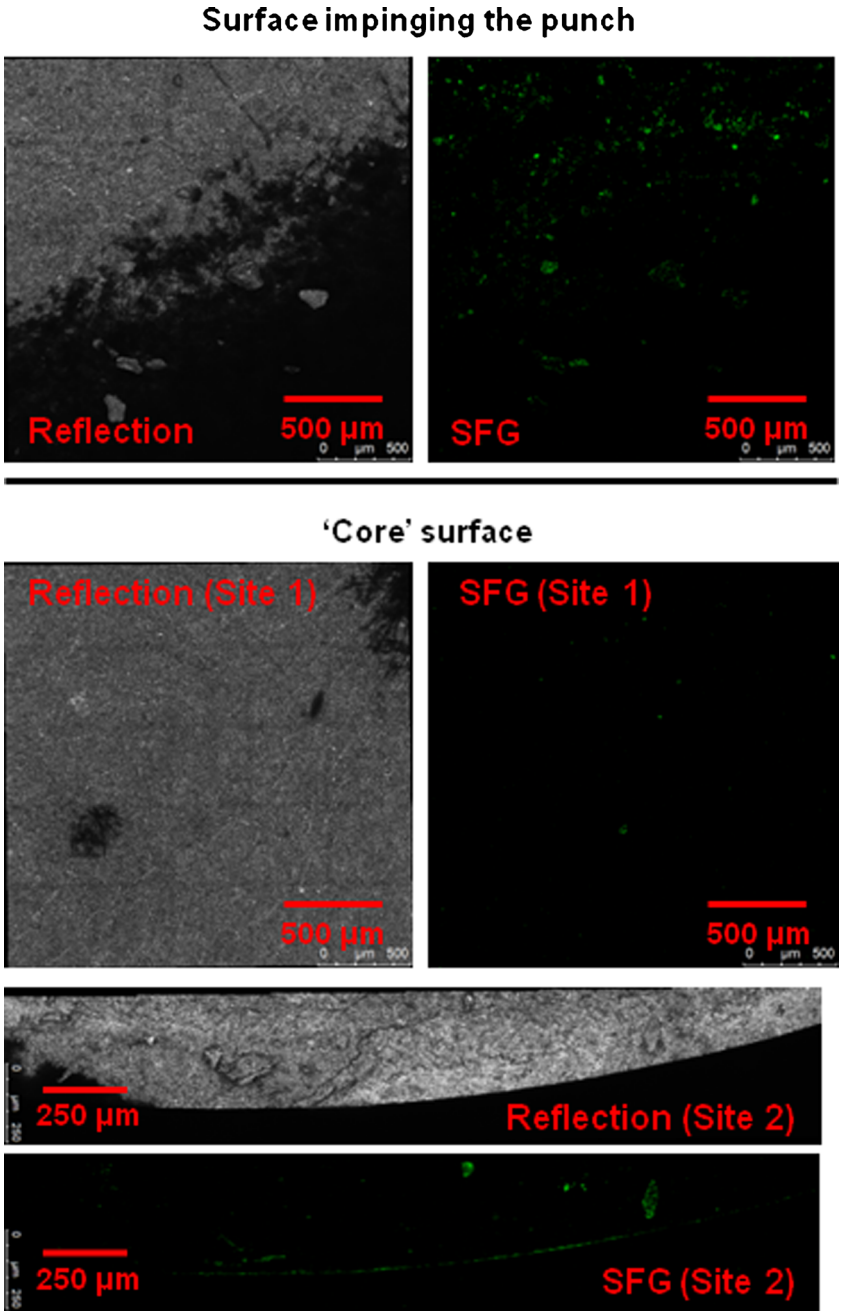

Figure 6 Reflection and SFG mosaic images of the surfaces of a tablet containing quench cooled mixture of silica and griseofulvin (1:1 w/w ratio) prepared using the configuration in Fig. 5a. Sites 1 and 2 of the 'core' surface cross-sections represent the regions in the middle and the edge of the tablet, respectively. The SFG signals (green) indicate crystalline regions.

cross-section images of the core of the tablets upon compression (i.e. Day 0) revealed that limited crystallinity was detected in the core of the tablets containing HPMCAS and MCC (Fig. 7). A faint green network of crystallinity was observed in the core of the tablet containing PEG indicating the extensive crystallization in the core of the tablet. Comparison of these results with those results of neat amorphous griseofulvin tablets without any excipients suggests that addition of HPMCAS and MCC did not have any effect on the compression-induced crystallization behavior of amorphous griseofulvin. PEG on the other hand, catalyzed the compression-induced crystallization process. No crystallinity features were detected in the SEM images of the surfaces and the core of the amorphous griseofulvin tablets containing various polymers upon compression (Figure S6).

Storing the sample for 2 days at 30°C/ 0%RH did not result in a noticeable progression in the crystallization of amorphous griseofulvin tablet containing HPMCAS as seen in Fig. 7. However, marked progression in crystallization upon storage was observed on the surface and also in the core of the amorphous griseofulvin tablet containing MCC. When these results were compared to those of neat amorphous griseofulvin tablets, the addition of HPMCAS seemed to delay the progression of crystallization upon storage in the core of the

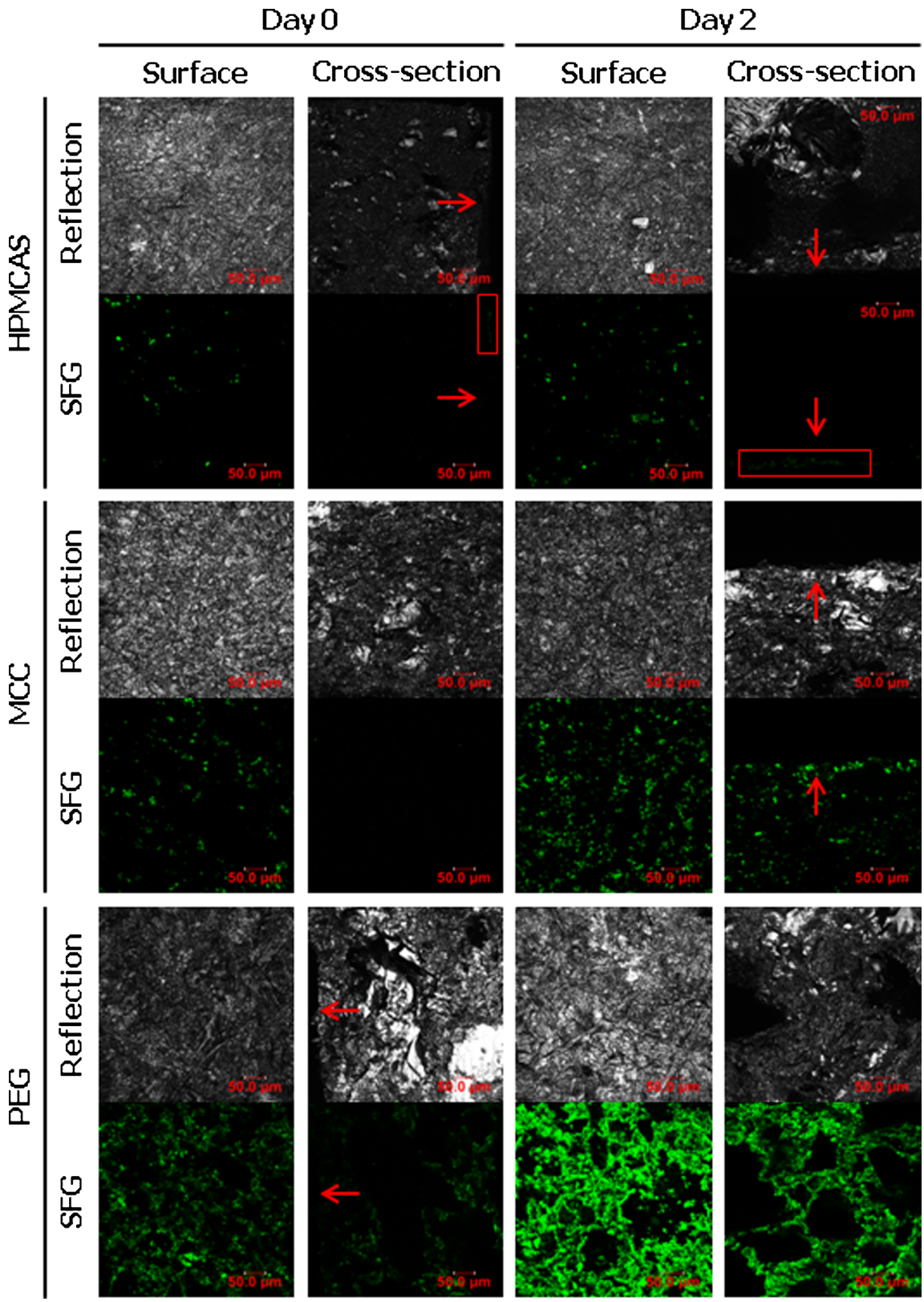

Figure 7 Reflection and SFG images of the surfaces and the cross-sections of tablets containing binary mixtures of neat amorphous griseofulvin and various polymers (1:1 w/w ratio) upon storage at 30°C/ 0%RH. The SFG signals (green) indicate crystalline regions. The red arrows indicate the surface edge of the tablets. The red rectangle highlights the region with low level of crystallinity (faint green). The scale bars indicate 50 μm.

tablet. MCC on the other hand, appeared to enhance the progression of crystallization upon storage of amorphous griseofulvin in the core of the tablet. The intensity of the SFG signal of the stored amorphous griseofulvin tablet containing PEG was much greater than the intensity of the SFG signal of the freshly prepared tablet. This observation is attributed to the lower and more superficial crystallinity at the beginning of the study giving rise to lower intensity. No noticeable crystalline features were detected in the SEM images of the stored amorphous griseofulvin tablets containing HPMCAS and MCC (Figure S6 (supporting information)). However, crystalline features were observed in the SEM images of the stored amorphous griseofulvin tablet containing PEG. The branch-like features observed on the surface of the tablet and the uneven surface of the cross-section of the amorphous griseofulvin tablets (Figure S6 (supporting information)) were indicative of crystalline features.

In order to further investigate the reason behind the observed inhibitory or catalytic effects of the various polymers on the crystallization process of amorphous griseofulvin in the form of a tablet, physical mixtures of the various polymers and neat amorphous griseofulvin were prepared and the evolution of the solid state of the amorphous griseofulvin particles upon storage was monitored using SFG microscopy. Figure 8 shows the SFG images and their corresponding reflection images of the physical mixtures upon preparation and also after being exposed to ambient conditions for 150 min. It can be seen that after 150 min of exposure to ambient conditions, crystallinity was only observed for the physical mixture containing PEG. This suggests the presence of PEG particles accelerated the crystallization process of neat amorphous griseofulvin particles. The specific mechanism behind this observation is currently not certain. A previous report suggests that PEG particles acted as heterogeneous nucleation sites for crystallization to occur (27).

There are many factors that could have contributed to the catalytic or inhibitory effects of the polymers on the crystallization of neat amorphous griseofulvin in the tablet and powder forms which include amorphous/semi-crystalline nature, particle size, compressibility and moisture content of the

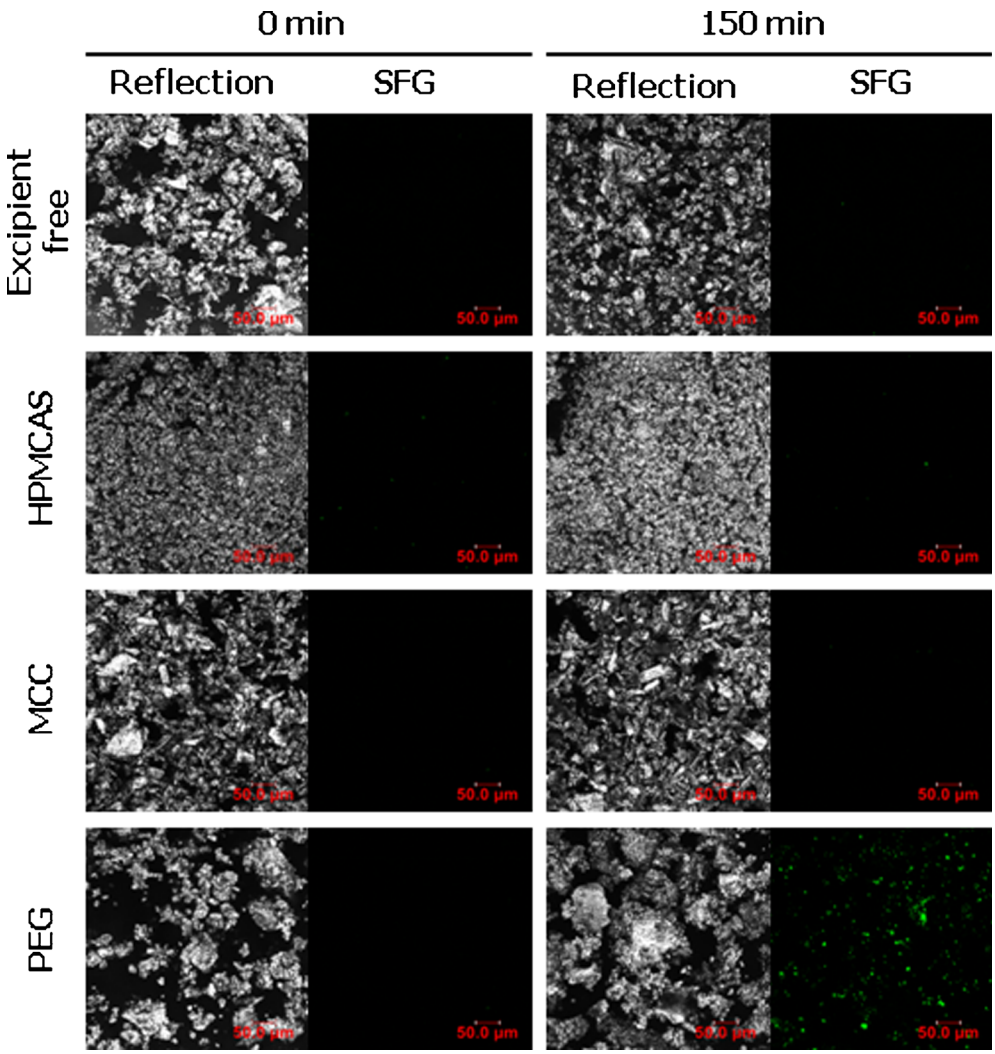

Figure 8 Reflection and SFG images of binary mixtures of neat amorphous griseofulvin and various polymers (1:1 w/w ratio) in the form of powder upon storage at ambient conditions. The SFG signals (green) indicate crystalline regions. The scale bars indicate 50 μm.

polymers. Thus, it is of great interest to carry out detailed investigations on the specific reasons for the crystallization modification rate of the various excipients on amorphous griseofulvin in the future. In any case, it is evident that the selection of appropriate excipients is crucial for the design of amorphous formulations with optimal physical stability.

As discussed in the introduction above, in order to efficiently generate sum-frequency signal, phase matching condition has to be fulfilled meaning that the excitation lasers need to combine in the right phase with the second order response. However, in case of strong focusing the phase matching conditions are relaxed because of the large cone of interfering waves and the short interaction length (23). With the focusing conditions used in this study the nonlinear intensity dependence restricts the excitation into the focal depth of the order of 1–2 μm.

The intensity of the SFG signal is also related to the crystal orientation with respect to the polarization direction of the excitation lasers. In our experiments the orientations of both the tablets and the formed crystals are random. We did not use the intensity for evaluation of the level of crystallinity but rather just estimated the overall area where any SFG was observed over the detection background level. Thus, it is unlikely that any significant part of crystalline material would have been missed due to a molecular orientation not emitting SFG signal.

Future investigations related to SFG microscopy include the analysis of crystallization kinetics in different types of drugs and amorphous materials due to other processing methods and during dissolution. In these studies the combined use of SFG and CARS microscopies is expected to help in resolving crystalline materials from amorphous materials. In addition, polarization sensitive detection could be used to further investigate the crystal organization.

CONCLUSIONS

SFG microscopy was successfully used in combination with ATR-FTIR spectroscopy and SEM to understand the crystallization behavior of neat amorphous griseofulvin tablets. Nonuniform crystallization was observed upon compression of neat amorphous griseofulvin with crystallization predominantly occurring on the surface of the tablets and minimal crystallization in the core of the tablets. The presence of excipients in the tablets was not able to mitigate the compression-induced surface crystallization of amorphous griseofulvin tablets. However, the addition of the excipients altered the crystallization rate of amorphous griseofulvin in the core of the tablets upon compression and storage. Thus, prudent consideration is needed when selecting and incorporating excipients for the formulation of amorphous dosage forms.

ACKNOWLEDGMENTS AND DISCLOSURES

This study was partially supported by the Pharmacy Grant 2013 (University of Helsinki). Elman Poole Travelling Fellowship and the University of Otago Doctoral Scholarship are gratefully acknowledged for providing Pei Ting Mah with financial support. Timo Laaksonen acknowledges funding from the Academy of Finland grant no. 258114.

REFERENCES

1. Lipinski CA. Drug-like properties and the causes of poor solubility and poor permeability. J Pharmacol Toxicol Methods. 2000;44(1):235–49.
2. Lipinski CA, Lombardo F, Dominy BW, Feeney PJ. Experimental and computational approaches to estimate solubility and permeability in drug discovery and development settings. Advanced Drug Deliv Rev. 2012;64, Supplement:4–17.
3. Elder DP, Holm R, Diego HL. Use of pharmaceutical salts and cocrystals to address the issue of poor solubility. Int J Pharm. 2013;453(1):88–100.
4. Kurkov SV, Loftsson T. Cyclodextrins. Int J Pharm. 2013;453(1):167–80.
5. Lu Y, Park K. Polymeric micelles and alternative nanonized delivery vehicles for poorly soluble drugs. Int J Pharm. 2013;453(1):198–214.
6. Möschwitzer JP. Drug nanocrystals in the commercial pharmaceutical development process. Int J Pharm. 2013;453(1):142–56.
7. Mu H, Holm R, Müllertz A. Lipid-based formulations for oral administration of poorly water-soluble drugs. Int J Pharm. 2013;453(1):215–24.
8. Kawakami K. Current status of amorphous formulation and other special dosage forms as formulations for early clinical phases. J Pharm Sci. 2009;98(9):2875–85.
9. Babu NJ, Nangia A. Solubility advantage of amorphous drugs and pharmaceutical cocrystals. Cryst Growth Des. 2011;11(7):2662–79.
10. Laitinen R, Löbmann K, Strachan CJ, Grohganz H, Rades T. Emerging trends in the stabilization of amorphous drugs. Int J Pharm. 2013;453(1):65–79.
11. Hancock BC, Zografi G. Characteristics and significance of the amorphous state in pharmaceutical systems. J Pharm Sci. 1997;86(1):1–12.
12. Yu L. Amorphous pharmaceutical solids: preparation, characterization and stabilization. Adv Drug Deliv Rev. 2001;48(1):27–42.
13. Ayenew Z, Paudel A, Rombaut P, Mooter G. Effect of compression on non-isothermal crystallization behaviour of amorphous indomethacin. Pharm Res. 2012;29(9):2489–98.
14. Thakral NK, Mohapatra S, Stephenson GA, Suryanarayanan R. Compression-induced crystallization of amorphous indomethacin in tablets: characterization of spatial heterogeneity by two-dimensional X-ray diffractometry. Mol Pharm. 2015;12(1):253–63.
15. Shah B, Kakumanu VK, Bansal AK. Analytical techniques for quantification of amorphous/crystalline phases in pharmaceutical solids. J Pharm Sci. 2006;95(8):1641–65.
16. Chieng N, Rades T, Aaltonen J. An overview of recent studies on the analysis of pharmaceutical polymorphs. J Pharm Biomed Anal. 2011;55(4):618–44.
17. Widjaja E, Kanaujia P, Lau G, Ng WK, Garland M, Saal C, *et al.* Detection of trace crystallinity in an amorphous system using

Raman microscopy and chemometric analysis. Eur J Pharm Sci. 2011;42(1–2):45–54.
18. Kanaujia P, Lau G, Ng WK, Widjaja E, Schreyer M, Hanefeld A, *et al.* Investigating the effect of moisture protection on solid-state stability and dissolution of fenofibrate and ketoconazole solid dispersions using PXRD, HSDSC and Raman microscopy. Drug Dev Ind Pharm. 2011;37(9):1026–35.
19. Lee CJ, Strachan CJ, Manson PJ, Rades T. Characterization of the bulk properties of pharmaceutical solids using nonlinear optics - a review. J Pharm Pharmacol. 2007;59(2):241–50.
20. Schneider L, Peukert W. Second harmonic generation spectroscopy as a method for in situ and online characterization of particle surface properties. Part Part Syst Charact. 2006;23(5):351–9.
21. Strachan CJ, Windbergs M, Offerhaus HL. Pharmaceutical applications of non-linear imaging. Int J Pharm. 2011;417(1–2):163–72.
22. Shen Y. Surface properties probed by second-harmonic and sum-frequency generation. Nature. 1989;337:519–25.
23. Zumbusch A, Holtom GR, Xie XS. Three-dimensional vibrational imaging by coherent anti-Stokes Raman scattering. Phys Rev Lett. 1999;82(20):4142.
24. Strachan CJ, Lee CJ, Rades T. Partial characterization of different mixtures of solids by measuring the optical nonlinear response. J Pharm Sci. 2004;93(3):733–42.
25. Chowdhury AU, Zhang S, Simpson GJ. Powders analysis by second harmonic generation microscopy. Anal Chem. 2016;88(7):3853–63.
26. Schmitt PD, Trasi NS, Taylor LS, Simpson GJ. Finding the needle in the haystack: characterization of trace crystallinity in a commercial formulation of paclitaxel protein-bound particles by Raman spectroscopy enabled by second harmonic generation microscopy. Mol Pharm. 2015;12(7):2378–83.
27. Zhu Q, Harris MT, Taylor LS. Modification of crystallization behavior in drug/polyethylene glycol solid dispersions. Mol Pharm. 2012;9(3):546–53.
28. Zhu Q, Toth SJ, Simpson GJ, Hsu H-Y, Taylor LS, Harris MT. Crystallization and dissolution behavior of naproxen/polyethylene glycol solid dispersions. J Phys Chem B. 2013;117(5):1494–500.
29. Wanapun D, Kestur US, Kissick DJ, Simpson GJ, Taylor LS. Selective detection and quantitation of organic molecule crystallization by second harmonic generation microscopy. Anal Chem. 2010;82(13):5425–32.
30. Wanapun D, Kestur US, Taylor LS, Simpson GJ. Single particle nonlinear optical imaging of trace crystallinity in an organic powder. Anal Chem. 2011;83(12):4745–51.
31. Kestur US, Wanapun D, Toth SJ, Wegiel LA, Simpson GJ, Taylor LS. Nonlinear optical imaging for sensitive detection of crystals in bulk amorphous powders. J Pharm Sci. 2012;101(11):4201–13.
32. Hsu H-Y, Toth SJ, Simpson GJ, Taylor LS, Harris MT. Effect of substrates on naproxen-polyvinylpyrrolidone solid dispersions formed via the drop printing technique. J Pharm Sci. 2013;102(2):638–48.
33. Mahieu A, Willart J-F, Dudognon E, Eddleston MD, Jones W, Danède F, *et al.* On the polymorphism of griseofulvin: identification of two additional polymorphs. J Pharm Sci. 2013;102(2):462–8.
34. Pan Q, Guo P, Duan J, Cheng Q, Li H. Comparative crystal structure determination of griseofulvin: powder X-ray diffraction versus single-crystal X-ray diffraction. Chin Sci Bull. 2012;57(30):3867–71.
35. Zoumi A, Yeh A, Tromberg BJ. Imaging cells and extracellular matrix in vivo by using second-harmonic generation and two-photon excited fluorescence. Proc Natl Acad Sci. 2002;99(17):11014–9.
36. Gallais L, Douti D-B, Commandre M, Batavičiūtė G, Pupka E, Ščiuka M, *et al.* Wavelength dependence of femtosecond laser-induced damage threshold of optical materials. J Appl Phys. 2015;117(22):223103.
37. Watanabe T, Wakiyama N, Usui F, Ikeda M, Isobe T, Senna M. Stability of amorphous indomethacin compounded with silica. Int J Pharm. 2001;226(1–2):81–91.
38. Wang L, Cui FD, Sunada H. Preparation and evaluation of solid dispersions of nitrendipine prepared with fine silica particles using the melt-mixing method. Chem Pharm Bull. 2006;54(1):37–43.
39. Hellrup J, Alderborn G, Mahlin D. Inhibition of recrystallization of amorphous lactose in nanocomposites formed by spray-drying. J Pharm Sci. 2015;104(11):3760–9.
40. Ellison CD, Ennis BJ, Hamad ML, Lyon RC. Measuring the distribution of density and tabletting force in pharmaceutical tablets by chemical imaging. J Pharm Biomed Anal. 2008;48(1):1–7.
41. De Figueiredo LP, Ferreira FF. The Rietveld method as a tool to quantify the amorphous amount of microcrystalline cellulose. J Pharm Sci. 2014;103(5):1394–9.
42. Takahashi Y, Tadokoro H. Structural studies of polyethers, $(-(CH2)_mO-)_n$. X. Crystal structure of poly (ethylene oxide). Macromolecules. 1973;6(5):672–5.
43. Pielichowska K, Głowinkowski S, Lekki J, Biniaś D, Pielichowski K, Jenczyk J. PEO/fatty acid blends for thermal energy storage materials. Structural/morphological features and hydrogen interactions. Eur Polym J. 2008;44(10):3344–60.